A&A 546, A123 (2012)
DOI: 10.1051/0004-6361/201118567

Astronomy & Astrophysics

Large distance of ε Aurigae inferred from interstellar absorption and reddening⋆,⋆⋆

E. F. Guinan[1], P. Mayer[2], P. Harmanec[2], H. Božić[3], M. Brož[2], J. Nemravová[2], S. Engle[1], M. Šlechta[4], P. Zasche[2], M. Wolf[2], D. Korčáková[2], and C. Johnston[1]

[1] Dept. of Astronomy & Astrophysics, Villanova University, 800 E. Lancester Ave., Villanova, PA 19085, USA
e-mail: Edward.Guinan@villanova.edu
[2] Astronomical Institute of the Charles University, Faculty of Mathematics and Physics, V Holešovičkách 2, 18000 Praha 8, Czech Republic
[3] Hvar Observatory, Faculty of Geodesy, University of Zagreb, 10000 Zagreb, Croatia
[4] Astronomical Institute, Academy of Sciences of the Czech Republic, 25165 Ondřejov, Czech Republic

Received 2 December 2011 / Accepted 16 July 2012

ABSTRACT

The long-period (P = 27.1 years) peculiar eclipsing binary ε Aur, which has recently completed its two year-long primary eclipse, has perplexed astronomers for over a century. The eclipse arises from the transit of a huge, cool and opaque, disk across the face of the F0 Iab star. One of the principal problems with understanding this binary is that the very small parallax of $p = (1.53 \pm 1.29)$ mas, implying a distance range of $d \sim (0.4–4.0)$ kpc, returned by a revised reduction of the HIPPARCOS satellite observations, is so uncertain that it precludes a trustworthy estimate of the luminosities and masses of the binary components. A reliable distance determination would help solve the nature of this binary and distinguish between competing models.

A new approach is discussed here: we estimate the distance to ε Aur from the calibration of reddening and interstellar-medium gas absorption in the direction of the system. The distance to ε Aur is estimated from its measured $E(B-V)$ and the strength of the diffuse interstellar band 6613.56 Å. Spectroscopy and *UBV* photometry of several B- and A-type stars (<1° of ε Aur) were carried out. The distances of the reference stars were estimated from either measured or spectroscopic parallaxes. The range in distances of the reference stars is from 0.2 to 3.0 kpc. We find reasonably tight relations among $E(B-V)$, EW, and I_c (6613 Å feature) with distance. From these calibrations, a distance of $d = (1.5 \pm 0.5)$ kpc is indicated for ε Aur. If ε Aur is indeed at (or near) this distance, its inferred absolute visual magnitude of $M_V \simeq (-9.1 \pm 1.1)$ mag for the F-supergiant indicates that it is a very young, luminous and massive star. Noteworthy, the high luminosity inferred here is well above the maximum value of $M_V \simeq -6\overset{m}{.}2$ expected for (less-massive) post asymptotic giant branch supergiant stars. Thus, based on the circumstantial evidence, the higher-mass model appears to best explain the properties of this mysterious binary system.

As a by-product of this study, our spectroscopy led to the finding that two of the stars used in the distance calibrations, HD 31617 and HD 31894, are newly discovered spectroscopic binaries, and HD 32328 is a new radial-velocity variable.

Key words. binaries: eclipsing – stars: AGB and post-AGB – stars: distances – stars: massive – stars: individual: eps Aurigae

1. Introduction

ε Aur (7 Aur, HR 1605, HD 31964) is a bright ($V \simeq 3\overset{m}{.}0$) single-line eclipsing binary with so far the longest known orbital period of 27.1 years ($9890\overset{d}{.}3$) (Ludendorff 1903; Stefanik et al. 2010; Chadima et al. 2010). The duration of the eclipse is almost 2 years and its last eclipse terminated by the end of August 2011. For the first time, interferometric observations carried out during the recent eclipse (see Kloppenborg et al. 2010) "imaged" the dark, flattened disk component transiting the F-supergiant star.

Two principal models of the system have been considered, often referred to as the high- and low-mass models (Guinan & DeWarf 2002, and references therein). Although they differ quite substantially from each other, the distances that follow from the rather uncertain HIPPARCOS parallax quoted in Table 1 do not allow to distinguish between the models from mainly luminosity considerations. In Table 1 we also summarize several other attempts to derive the parallax of ε Aur. The true nature of this unusual eclipsing binary remains a puzzle in spite of many attempts to explain its properties. As noted previously, one of the principal problems is that the very small parallax returned by the HIPPARCOS satellite is so uncertain that it precludes a trustworthy estimate of the luminosities and thus masses of the binary components. A reliable distance determination would help solve the nature of this binary and distinguish between the competing models that explain this extraordinary binary system.

According to the high-mass model, first considered by Kuiper et al. (1937) and later developed by Carroll et al. (1991), the F-supergiant component is a normal high mass/high luminosity Pop. I supergiant and its mysterious cool disk (+ star) companion is either a very young, high mass object that has accreted gas from the F-supergiant or a pre-Main Sequence star with circumstellar material.

In the low mass model, first suggested by Eggleton & Pringle (1985) and by Lambert & Sawyer (1986) and recently advocated by Hoard et al. (2010), the F-supergiant is a post-asymptotic giant branch (AGB) star, of low to moderate mass (initial mass

⋆ Based on new spectral and photometric observations from the Hvar, Ondřejov and Tautenburg Observatories, the Four College Automatic Photoelectric Telescope and from the ESA HIPPARCOS satellite.

⋆⋆ Appendices are available in electronic form at http://www.aanda.org

Table 1. Various determinations of the parallax of ε Aur.

Source	p (mas)	Notes
Adams & Joy (1917)	11–22	1
Adams & Joy (1917)	60	2
Strand (1959)	6 ± 4	3
Strand (1959)	1	4
van de Kamp & Lippincott (1968)	4 ± 2	5
van de Kamp (1978)	1.72 ± 0.08	4
Heintz & Cantor (1994)	3 ± 2	6
Heintz & Cantor (1994)	1.65 ± 0.15	4
Perryman & ESA (1997)	1.60 ± 1.16	7
van Leeuwen (2007a,b)	1.53 ± 1.29	8

Notes. Trigonometric parallaxes are quoted unless specified otherwise. 1... spectroscopic parallax; 2... by Jewdokimow at Yerkes; 3... 59 nights, Yerkes 1926−58; 4... comparing the semi-major axis from the astrometric and spectroscopic solutions; 5... 174 obs. at Sproul in 1938−56; 6... an extended series of the Sproul 363 night means over 44 years; 7... original HIPPARCOS parallax; 8... revised reduction of HIPPARCOS parallaxes.

Table 2. Equatorial coordinates and spectral types of ε Aur and the calibration stars in its neighbourhood.

Star	α (J2000.0)	δ (J2000.0)	Sp. type	Note
ε Aur	$5^h01^m58\overset{s}{.}13245$	$43°49'23\overset{''}{.}9059$	F0Ia	
HD 31617	$4^h59^m21\overset{s}{.}24899$	$43°19'24\overset{''}{.}1690$	B2IV	1
HD 31894	$5^h01^m34\overset{s}{.}29127$	$43°26'08\overset{''}{.}6252$	B2IV-V	2
HD 32328	$5^h04^m32\overset{s}{.}73112$	$43°43'39\overset{''}{.}5641$	B8V	1
HD 277197	$5^h01^m11\overset{s}{.}5460$	$43°34'41\overset{''}{.}915$	B3V	3
BD+43°1168	$5^h02^m12\overset{s}{.}374$	$43°51'42\overset{''}{.}35$	B9Iab	

Notes. 1... newly discovered SB1; 2... newly discovered SB2; 3... the spectral class estimated by us.

≈1−7 $M_\odot$; final (current) mass <1.0 $M_\odot$). In this model, the large, cool disk binary component resulted from the recent capture of gas from a prior large mass-loss/transfer phase from the F-supergiant.

2. A methodology of the distance calibration

We initially selected three stars close in the sky to ε Aur, HD 31617, HD 31894, and HD 277197, because they all have similarly small space motions and reddening values as ε Aur itself. We thought that these stars, together with ε Aur, could be the brighter members of a young stellar association. Even though this could be the case, the errors in their proper motions and spectroscopic distance estimates preclude drawing definite connection. But if this were the case, this would imply a distance to ε Aur of about 1.1 kpc (see Table 10).

We decided to try an alternative approach to the problem. On the premise that the interstellar medium in the direction of ε Aur has similar properties as in the surrounding directions (within a few degrees around ε Aur) as projected onto the sky, we selected several stars closer than 1° to ε Aur in the sky (and accessible to the telescopes available to us) and obtained their spectra and *UBV* photometry. The list of these stars is in Table 2.

Infrared data from DIRBE/COBE (Schlegel et al. 1998) confirm that our assumption is valid – the calibration stars are located at positions, where the dust thermal emission (summed along the line of sight) is indeed comparable (see Fig. 1).

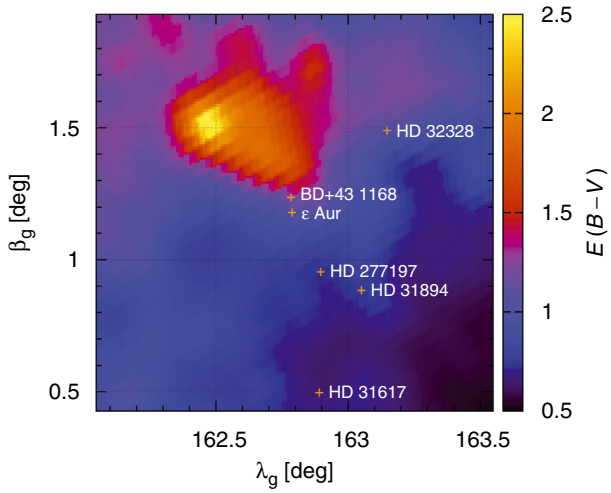

Fig. 1. Reddening $E(B-V)$ computed from IR emission for *extragalactic* sources as a function of galactic coordinates. The data were taken from Schlegel et al. (1998). Our calibration stars and ε Aur are denoted by crosses. The values of $E(B-V)$ range from 0.65 to 1.22 for the positions of the calibration stars (note that these are *not* $E(B-V)$ for the stars themselves). The cloud visible in the north-east direction is the nebular region TGU H1105 (Dobashi et al. 2005).

Table 3. Comparison of the $E(B-V)$ and $E(V-K)$ reddening for our calibration stars in the neighbourhood of ε Aur.

Star	$E(B-V)$	$E(V-K)$	$E(V-K)/E(B-V)$
HD 31617	0.25	0.63	2.52
HD 31894	0.27	0.74	2.74
HD 32328	0.06	0.19	3.17
HD 277197	0.26	0.73	2.82
BD+43°1168	0.90	2.46	2.74

Notes. See the text for details.

Using the data from the 2MASS catalogue, it is possible to calculate the ratio $E(V-K)/E(B-V)$ for all calibration stars (see Table 3). Comparison of these data with the values derived by Koornneef (1983) also clearly shows that the extinction of these stars is normal (cf. Table 4 of Johnson 1965).

Using the measured parallaxes or spectroscopically estimated distances to these stars, we attempted to derive two independent *calibration relations*: (1) the distance d as a function of the strength of the diffuse interstellar band (DIB) at 6613.56 Å, and (2) the distance d as a function of the $E(B-V)$ reddening. The idea is to use these calibrations for a new estimate of the distance to ε Aur. It is worth noting that a smooth dependence of the reddening on the distance in the region near ε Aur has already been found by McCuskey (1949), based on photographic spectra and magnitudes. There are several studies of the strength and shape of the DIB at 6613 Å in the recent literature (cf., e.g. Jenniskens & Desert 1994; Galazutdinov et al. 2008; Hobbs et al. 2009; McCall et al. 2010) but we were unable to find any published calibration of this feature vs. distance. Munari et al. (2008) found a tight relation between the EW of another DIB at 8620.4 Å and $E(B-V)$ and another, though a less perfect such relation was also published for the DIB at 5780.5 Å by McCall et al. (2010). The latter authors also found a very good correlation between the EWs of 6613.6 and 6196.0 DIBs. Unfortunately, none of these additional DIBs are covered by our spectra. The limited spectral resolution of our spectra may imply that our EWs only represent a lower limit to the true EW

of the 6613 DIB but in the light of the above-mentioned studies we do believe that with a homogeneous series of the spectra taken with the same instrument a calibration of the 6613 DIB vs. distance within a limited area in the sky should be feasible.

Details of all spectral observations, their reduction and radial-velocity (RV hereafter) measurements can be found in Appendix A, while the photoelectric *UBV* observations and their reductions are described in Appendix B.

For each of the calibration stars we proceed as follows: (i) using the observed spectra, we derive $T_{\rm eff}$, $\log g$ by matching the synthetic spectra; (ii) using a modern stellar-evolution code, we determine the corresponding mass $m_\star$ and luminosity L which enables us to compute the distance. We now describe the procedure in more details.

One of us, JN, has developed a program, which derives the optimal values of the effective temperature $T_{\rm eff}$, logarithm of the gravitational acceleration $\log g$, projected rotational velocity $v \sin i$ and RV via interpolation in a grid of synthetic spectra and minimalization of the sum of squares of O−C between the observed and interpolated synthetic spectrum. For multiple systems of N components, it also derives the relative luminosities of the components, preserving the constraint that $\sum_{j=1}^{N} L_i = 1$[1]. For practical applications, we used the grid of recent elaborated synthetic spectra published by Lanz & Hubeny (2007) (Bstar grid hereafter). We assumed a (fixed) value of metallicity $Z = 0.04$ corresponding to massive and consequently young stars.

Realistic uncertainties of the best-fit effective temperatures are of the order $\Delta T_{\rm eff} \simeq 1000$ K for hot stars (with $T_{\rm eff} \gtrsim 20\,000$ K) and down to 100 K for cooler stars ($T_{\rm eff} \lesssim 10\,000$ K). For $\log g$ we typically have an uncertainty of about $\Delta \log g \simeq 0.5$.

We also adopted Lanz & Hubeny (2007) bolometric corrections BC, interpolating for the optimal values of $T_{\rm eff}$ and $\log g$. Their BCs have a zero point defined by adopting the $\mathrm{BC}_\odot = -0\overset{\mathrm{m}}{.}07$. Following Torres (2010), we therefore adopted the observed Johnson V magnitude of the Sun, $V_\odot = -26\overset{\mathrm{m}}{.}76 \pm 0\overset{\mathrm{m}}{.}03$ and the distance modulus $V_\odot - M_{V\odot} = -31\overset{\mathrm{m}}{.}572$. For a comparison with evolutionary models, it is therefore necessary to adopt $M_{\rm bol\odot} = M_{V\odot} + \mathrm{BC}_\odot = 4\overset{\mathrm{m}}{.}742$.

To obtain reasonable estimates of the masses and bolometric magnitudes of the calibration stars, we used the stellar-evolution module `MESAstar` by Paxton et al. (2011)[2]. We took the optimal values of $T_{\rm eff}$ and $\log g$ (with their uncertainties) from the modelling of synthetic spectra and we searched for the corresponding initial mass $m_\star$ (range of masses) of the star for which evolutionary tracks are compatible with the parameters ($\log T_{\rm eff}$, $\log g$) inferred above. We assumed initial helium abundance $Y = 0.320$, metallicity $Z = 0.040$, and the mixing-length parameter $\alpha = 2.0$.

As we shall see later, we usually obtain the values of $\log g = 4.0$ to 4.5 which correspond to stars located at the main sequence. Note that main-sequence stars are neither very sensitive to the value of α nor to the selected wind scheme. The major source of uncertainty in $m_\star$ is thus the uncertainty of the effective temperature $T_{\rm eff}$.

Given the values of $m_\star$ and evolutionary tracks in the HR diagram ($T_{\rm eff}$, $\log L$) for all calibration stars, we can easily take the luminosities $\log L$ or bolometric magnitudes $M_{\rm bol} = M_{\rm bol\odot} - 2.5 \log L$ and determine the (spectroscopic) distances and their uncertainties.

In case the calibration star is a binary (as HD 31894) we can use the secondary as an independent check, with the mass ratio inferred from the RV curve being a strong additional constraint.

For the B9 Iab supegiant BD+43°1168, we adopted the unreddened $(B-V)_0$ index from the Johnson (1958) study. To obtain the dereddened V_0 magnitudes of all considered stars, we adopted the formula from Chap. 15 of Cox (2000)

$$V_0 = V - E(B-V) \cdot (3.30 + 0.28(B-V)_0 + 0.04E(B-V)) . \quad (1)$$

This way, our distance scale can contain a small systematic error but it should be internally consistent for all considered stars.

In the following sections, we first discuss the new observations and our detailed analyses of the individual calibration stars, then we establish the $d(EW)$, $d(I_{\rm c})$ and $d(E(B-V))$ calibrations, we derive appropriate 6613 Å line strengths and a range of $E(B-V)$ values for ε Aur and finally apply them to ε Aur.

3. The B type binary HD 31894

HD 31894 (BD+43°1164, HIP 23375) was classified B2IV-V by Walborn (1971). Danziger et al. (1967) included HD 31894 in their study of stars in the neighbourhood of the hydrogen-poor star HD 30353 in an effort to derive the distance to it. They studied the RVs and equivalent widths of the interstellar Na I and also interstellar polarization as a function of the distance. For HD 31894, they obtained $E(B-V) = 0\overset{\mathrm{m}}{.}27$ and adopted the distance modulus $m - M = 10.8$, but from their mean curve through the dependence of interstellar polarization on the distance modulus, the modulus of HD 31894 should be less than 9, while from their mean curve distance vs. equivalent width of the sodium D_1 and D_2 lines, the modulus should be about 9.3.

The absolute visual magnitude of HD 31894 was estimated from the measured equivalent width of the Hγ line in two studies: Petrie & Lee (1966) obtained $M_{\rm V} = -1\overset{\mathrm{m}}{.}7$ while Walborn (1971) found $M_{\rm V} = -2\overset{\mathrm{m}}{.}9$. Carnochan (1986) studied the interstellar 2200 Å feature for a number of stars including HD 31894, adopting the following *UBV* values from Deutschman et al. (1976):

$$V = 8\overset{\mathrm{m}}{.}41,\ B-V = 0\overset{\mathrm{m}}{.}04,\ U-B = -0\overset{\mathrm{m}}{.}66,\ \text{and}\ E(B-V) = 0\overset{\mathrm{m}}{.}28.$$

To derive the fundamental properties of HD 31894 more precisely, we began observing the star spectroscopically with the Ondřejov 2-m telescope and photometrically with the 0.65-m reflector at Hvar and later also with the 0.75-m Four-College Automatic Photoelectric Telescope (APT). One echelle spectrogram was kindly obtained and preliminarily reduced for us by Dr. Holger Lehmann with the Tautenburg Observatory 2-m reflector on JD 2 455 670.3.

To our surprise, already the first spectrum showed that the object is *a double-lined spectroscopic binary* and the second spectrum revealed a RV separation of 300 km s^{-1} between the B2 primary and a secondary of some later B spectral subclass.

3.1. The orbital period and orbital solution

After accumulating some 12 spectra, we were able to find out that the correct orbital period must be slightly longer than 11 days. It also turned out that the orbit has a high eccentricity. We then used the program `PHOEBE` (Prša & Zwitter 2005, 2006) to derive the orbital solution which is presented in Table 4.

Dr. Alan H. Batten kindly found and communicated to us the mid-exposure times of the old DAO spectrograms, for which

[1] By the relative luminosity we understand as usually the ratio $L_j / \sum_{j=1}^{N} L_j$ ($j = 1...N$) of the luminosities of individual components measured in physical units (outside the eclipses for the eclipsing systems).

[2] The latest release 3918 from April 2012.

Table 4. Orbital solution for HD 31894 derived in PHOEBE.

Element	Unit	Value with error
P	(d)	11.0459 ± 0.0051
$T_{\rm periastr.}$	(RJD)	$55\,601.864 \pm 0.022$
$T_{\rm super.c.}$	(RJD)	$55\,601.431 \pm 0.022$
e		0.6183 ± 0.0089
ω	(°)	154.10 ± 0.73
$a \sin i$	($R_\odot$)	39.68 ± 0.39
γ	(km s^{-1})	-1.82 ± 0.47
K_1	(km s^{-1})	85.6 ± 1.5
K_1/K_2		0.5879 ± 0.0093
K_2	(km s^{-1})	145.6 ± 2.6
$M_1 \sin^3 i$	($M_\odot$)	4.33 ± 0.13
$M_2 \sin^3 i$	($M_\odot$)	2.55 ± 0.08
χ^2		37.60
No. of RVs		19+19

Notes. The epochs are in RJD = HJD – 2 400 000.

Table 5. Orbital solution for the old DAO spectra of HD 31894 derived in PHOEBE.

Element	Unit	Value with error
P	(d)	11.0459 fixed
$T_{\rm periatr.}$	(RJD)	$31\,743.29 \pm 0.10$
γ	(km s^{-1})	-8.8 ± 3.9
χ^2		1.842
No. of RVs		4

Notes. All elements, besides the epoch and systemic velocity, were kept fixed from the solution for the new data – see Table 4. The epochs are in RJD = HJD – 2 400 000.

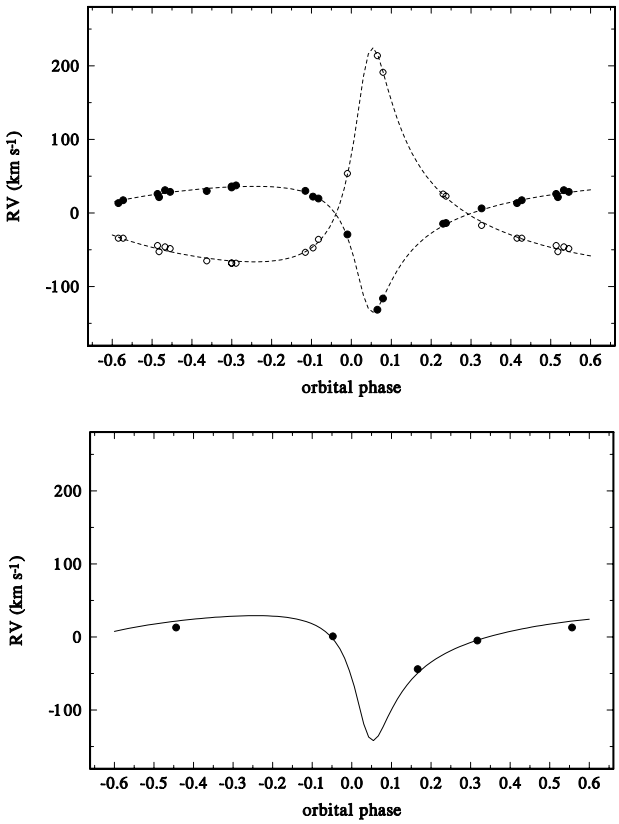

Fig. 2. Orbital radial-velocity curves of HD 31894 for the orbital period of 11$^{\rm d}$.0459. Phase zero corresponds to the superior conjunction. *Upper panel*: RV curves of the primary (filled circles) and secondary (open circles) and the PHOEBE solution calculated curves. *Bottom panel*: the RV curve based on the old DAO RVs.

the RVs were derived by Petrie & Pearce (1961). We calculated the corresponding heliocentric Julian dates and reproduce these RVs also in Table A.2.

Keeping the orbital elements fixed from the solution for our new RVs, we derived a separate solution for the old RVs, deriving only the epoch of periastron and the systemic velocity. The result is in Table 5 and the corresponding RV curve is shown in the lower panel of Fig. 2. Assuming that 2159, 2160 or 2161 orbital cycles elapsed between the old and new periastron epoch, we obtain the following possible values of the orbital period: 11$^{\rm d}$.0508, 11$^{\rm d}$.0456, and 11$^{\rm d}$.0405, respectively[3]. It is seen that after another season of observations, the accuracy of the orbital period derived from the new data would be sufficient to discriminate safely between the above three possible values of the orbital period. It is not clear, however, how significant the difference in the systemic velocity between the old and new RVs is. It is conceivable that some of the old RVs are actually slightly affected by the blending of the spectral lines of the primary and secondary. For the purpose of this study, we *have not* combined the old and new RVs to obtain a joint orbital solution. All subsequent discussion will be based on the orbital elements derived from the new spectra only – cf. Table 4 – and on the following ephemeris

$$T_{\rm super.conj.} = {\rm HJD}\ 2\,455\,601.431 + 11^{\rm d}.0459 \times E. \quad (2)$$

3.2. Properties of the binary system and its components

Our photometric observations safely excluded the possibility of binary eclipses. This means that we are not able to obtain a unique solution and that some assumptions must be made. Nevertheless, the observational data we accumulated allow us to obtain reasonable estimates.

In spite of a limited number of available spectra, we tentatively disentangled them, using the KOREL program (Hadrava 1995, 1997, 2004b, 2005). It converged to a solution closely similar to that of Table 4 and provided the disentangled spectra of both binary components. For the final disentangling, we kept the orbital elements of Table 4 fixed and obtained the disentangled spectra in the following three spectral regions: 6327–6422 Å, 6422–6645 Å, and 6630–6750 Å. For the second region containing Hα, we also allowed KOREL to disentagle and remove the telluric lines.

Comparing the disentagled spectra of the primary and secondary normalized to the joint continuum of both stars with synthetic spectra from the Bstar grid using the program by JN, discussed above, we obtained the *formally* best fit for the following values:

$T_{\rm eff} = 23\,490$ K, $\log g = 4.30$, $v \sin i = 74.4$ km s^{-1}, $L_1 = 0.809$,

and

$T_{\rm eff} = 17\,810$ K, $\log g = 4.52$, $v \sin i = 26.9$ km s^{-1}, $L_2 = 0.191$

for the primary and secondary, respectively. A comparison of the disentangled spectra with the interpolated synthetic ones is shown in Fig. 3 for the primary and in Fig. 4 for the secondary. The value of $\log g$ of 4.5 [cgs] is too high even for the zero-age main sequences stars. We verified that fixing $\log g = 4.25$ for both stars increases the χ^2 of the fit by only 2 per cent, leading

[3] Note that propagating the errors of both epochs does alter the quoted period values only on the fourth decimal digit.

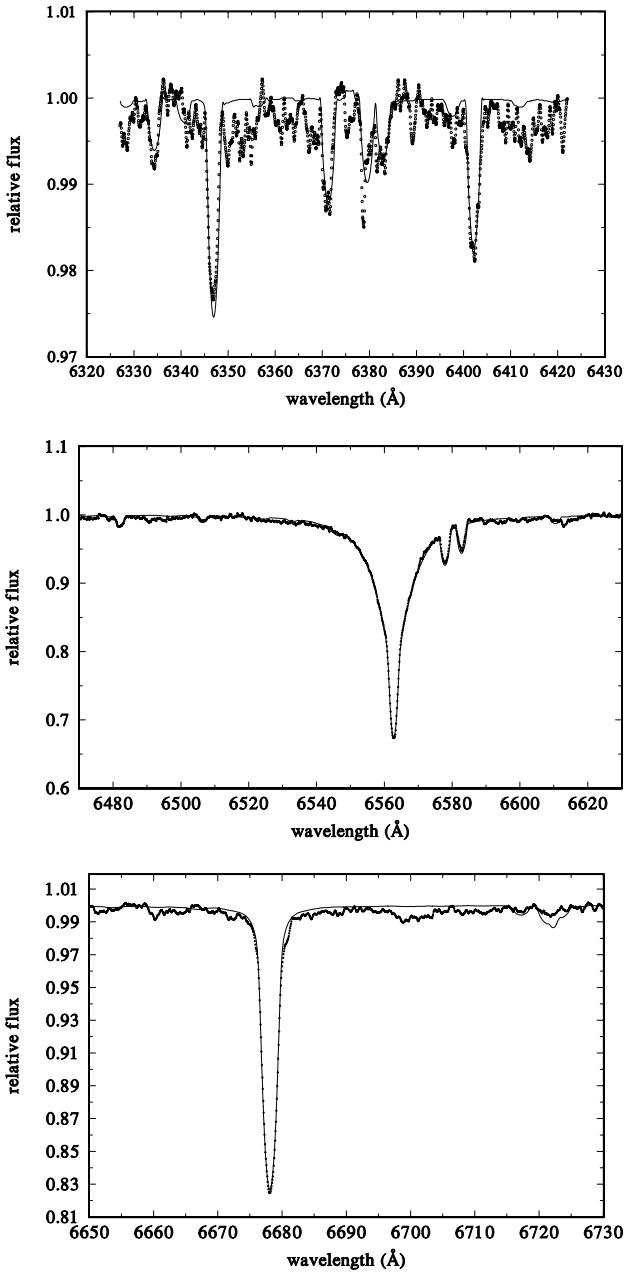

Fig. 3. A comparison of the disentangled line spectrum of the HD 31894 primary with a synthetic spectrum interpolated from the Bstar grid for $T_{\rm eff}$ = 23 490 K, log g = 4.30 [cgs] and v sin i = 74.4 km s^{-1} in three spectral segments containing stronger stellar lines. In all cases, dots denote the observed spectrum, while the synthetic spectra, shifted for the systemic velocity of −2 km s^{-1}, are shown as thin lines. A relative luminosity of the primary of L_1 = 0.809 was adopted for the comparison.

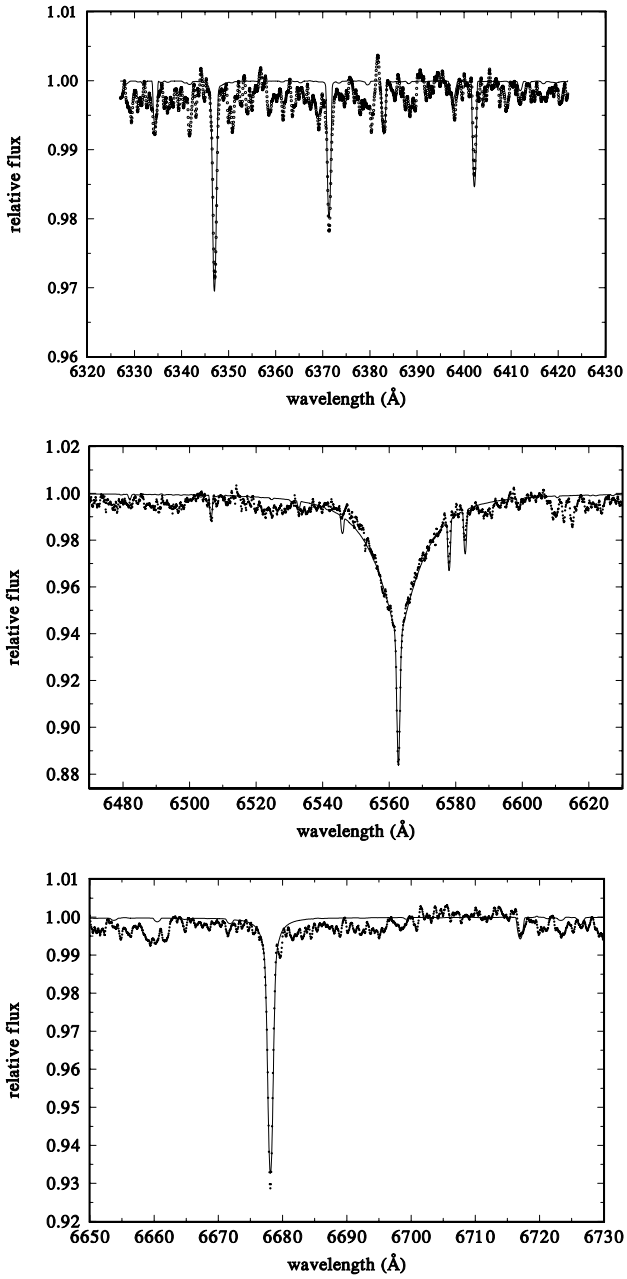

Fig. 4. A comparison of the disentangled line spectrum of the HD 31894 secondary with a synthetic spectrum interpolated from the Bstar grid for $T_{\rm eff}$ = 17 810 K, log g = 4.52 [cgs] and v sin i = 26.9 km s^{-1} in three spectral segments containing stronger stellar lines. In all cases, dots denote the observed spectrum, while the synthetic spectra, shifted for the systemic velocity of −2 km s^{-1}, are shown as thin lines. A relative luminosity of the secondary of L_2 = 0.191 was adopted for the comparison.

to lower $T_{\rm eff}$ of 22 800 and 17 000 K for the binary components. This confirms our estimate of typical uncertainties mentioned earlier.

In the next step we used the stellar-evolution module `MESAstar` by Paxton et al. (2011) to reproduce the observed $T_{\rm eff}$ and log g of the HD 31894 primary. Using the mass ratio from our orbital solution, we then estimated the range of masses for the secondary and calculated also its evolution to see how consistent the model and observed properties of the secondary will be for the same evolutionary age as for the primary. The evolutionary tracks are shown in Fig. 5.

We again used `PHOEBE` and, keeping the orbital elements fixed at the values of Table 4 but setting i = 50.°0, we included our *UBV* photometry and tuned the radii within reasonable limits to obtain the relative luminosity of the primary L_1 = 0.81 in the V band. The fit with `PHOEBE` led to the following *UBV* magnitudes at maximum light

$$V_{1+2} = 8.^{\rm m}499, \quad B_{1+2} = 8.^{\rm m}543, \quad \text{and} \quad U_{1+2} = 7.^{\rm m}898.$$

Using these values and the relative luminosities in all three passbands derived with `PHOEBE` (0.81, 0.82, and 0.84 in V, B, and U, respectively), we obtained the *UBV* magnitudes of both stars, and their standard dereddening led to the values presented in

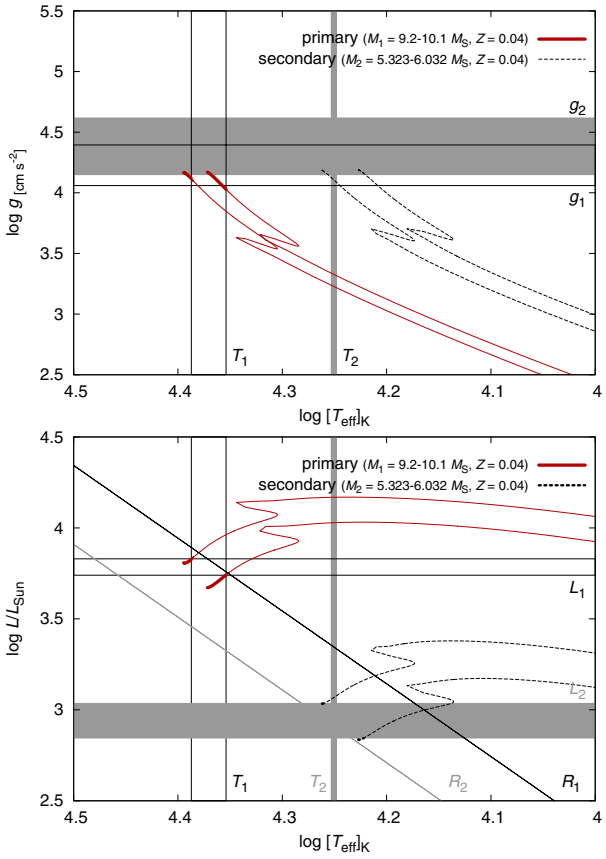

Fig. 5. Computed evolutionary tracks of both binary components of HD 31894 in a log g vs. $T_{\rm eff}$ diagram and in the HR diagram. See the text for details.

Table 6. Dereddened magnitudes of both binary components based on the PHOEBE fit.

Star	$E(B-V)$	$E(U-B)$	V_0	$(B-V)_0$	$(U-B)_0$
prim.	0.268	0.196	7.854	–0.233	–0.874
sec.	0.270	0.198	9.443	–0.183	–0.685

Notes. See the text for details.

Table 6. For illustration, the V-band light curve is shown in Fig. 6.

For the adopted range of effective temperatures of the primary from 23 000 to 24 000 K and of the secondary: 17 000–18 000 K, and estimating the range of bolometric magnitudes from the evolutionary calculations, one gets the ranges of the absolute visual magnitudes from $-2\overset{\rm m}{.}23$ to $-2\overset{\rm m}{.}55$ for the primary, and from $-0\overset{\rm m}{.}70$ to $-1\overset{\rm m}{.}32$ for the secondary. Combined with the dereddened V_0 magnitudes from Table 6 this gives the range of distances 1037–1202 pc for the primary, and 1066–1420 pc for the secondary. Weighting more the values for the primary, we adopt $d = 1150 \pm 150$ pc for the distance of the HD 31894 binary.

The radii we used in PHOEBE to fit the relative luminosities in the V band are

$$R_1 = 5.14\,R_\odot \quad \text{and} \quad R_2 = 3.12\,R_\odot.$$

4. The B star HD 31617

A relatively little studied B star HD 31617 (BD+43°1147, HIP 23186) is another object close to ε Aur in the sky. It was

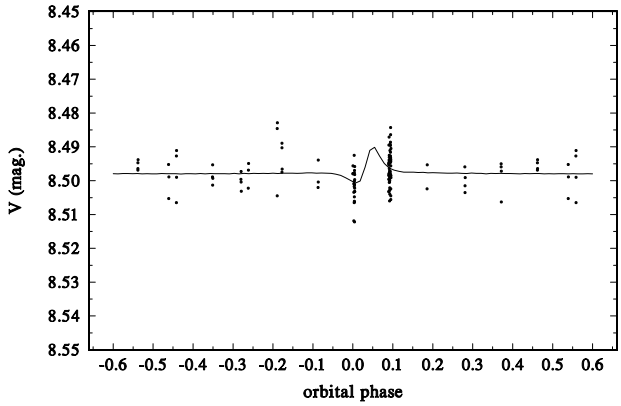

Fig. 6. Orbital V-band light curve of HD 31894 for the orbital period of $11\overset{\rm d}{.}0459$, based on a slightly more accurate APT individual observations. Phase zero corresponds to the superior conjunction. The PHOEBE solution, shown as a solid line, clearly exhibits the proximity effects near the periastron passage.

classified as B2IV by Hiltner (1956), who also obtained the following *UBV* values

$$V = 7\overset{\rm m}{.}42, \quad B-V = 0\overset{\rm m}{.}00, \quad U-B = -0\overset{\rm m}{.}77,$$

while Bouigue (1959) obtained

$$V = 7\overset{\rm m}{.}35, \quad \text{and} \quad B-V = 0\overset{\rm m}{.}00$$

as a mean of 3 individual observations. Plaskett & Pearce (1931) obtained 4 RVs at the Dominion Astrophysical Observatory (DAO) in 1924–1929 with a mean value of +3.5 km s^{-1} and a range over 10 km s^{-1}. The new reduction of the HIPPARCOS data by van Leeuwen (2007a,b) resulted in a negative value of the parallax. Therefore, no reliable trigonometrically measured distance to HD 31617 is available. However, Danziger et al. (1967) studied several stars near the hydrogen-poor star HD 30353 in an effort to derive its distance modulus via polarization mesurements by Hiltner and via the strength of the Na I interstellar line. For HD 31617, they obtained a modulus of 9.6 mag from polarimetry, and 10.0 mag from the strength of the interstellar lines, which implies distances of 832 and 1000 pc, respectively. Savage et al. (1985) investigated excess ultraviolet extinction for a number of B stars and did not find any for HD 31617.

We obtained 13 individual standard *UBV* observations at Hvar. The star was also used as a check star for observations of HD 31894 at Villanova and 34 *UBV* observations were secured. There are also 97 $H_{\rm p}$ observations secured by the HIPPARCOS satellite (Perryman & ESA 1997). None of these datasets show any significant light variability of this star. The mean standard Hvar values are in Table 9.

We succeded to secure 10 red Ondřejov spectra. The RV measurements of four good and sharp lines in SPEFO soon showed that the object is another single-line spectroscopic binary, for which we tentatively estimate an orbital period of about 60 d and a highly eccentric orbit. We use the inverse square of the rms errors of the mean RV of the four measured lines (Hα, He I 6678 Å and the C II doublet at 6578 & 6582 Å) for each measured spectrum to derive the weights of individual mean RVs. Our RV measurements, together with the low rms errors (mostly below 0.5 km s^{-1}) are reproduced in detail in Table A.3. We also tabulate there the old DAO RVs, for which we derived the heliocentric Julian dates. Regrettably, their phase distribution does not allow to improve the value of the orbital

Table 7. Orbital solution for HD 31617 derived in FOTEL.

Element	Unit	Value with error
P	(d)	59.2 ± 2.5
$T_{\rm periastr.}$	(RJD)	$56\,015.39 \pm 0.50$
$T_{\rm super.c.}$	(RJD)	56 028.45
e		0.759 ± 0.043
ω	(°)	295 ± 12
γ	(km s^{-1})	-4.79 ± 0.81
K_1	(km s^{-1})	16.9 ± 4.9
$f(M)$	($M_\odot$)	0.00815
rms	(km s^{-1})	0.680
No. of RVs		10

Notes. The epochs are in RJD = HJD – 2 400 000 and the rms is the standard error of 1 observation of unit weight.

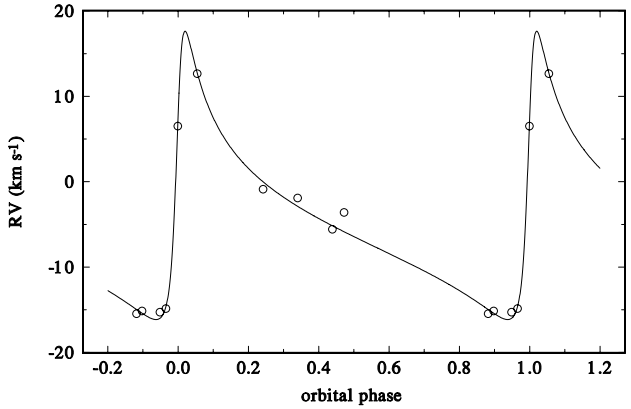

Fig. 7. Orbital radial-velocity curves of HD 31617 for the orbital period of 59$^{\rm d}$.2. Phase zero corresponds to the superior conjunction.

period. A preliminary orbital solution derived with the program FOTEL (Hadrava 1990, 2004a) are presented in Table 7.

We disentangled the spectrum of the primary with KOREL and the comparison with the Bstar grid returned the following values:

$$T_{\rm eff} = 24\,519\ {\rm K},\ \log g = 3.863\ [{\rm cgs}],\ \text{and}\ v\ \sin\ i = 32.3\ {\rm km\,s^{-1}}.$$

A comparison of the disentangled spectrum with the synthetic one is in Fig. C.1 in Appendix C. Evolutionary tracks bracketing the above values are shown in Fig. C.4 in Appendix C. They imply the mass of the HD 31617 primary in the range of 9.5 to 15 $M_\odot$, the bolometric magnitude between $-4\overset{\rm m}{.}36$ and $-7\overset{\rm m}{.}36$ and the absolute visual magnitude between $-2\overset{\rm m}{.}06$ and $-4\overset{\rm m}{.}88$. Together with $V_0 = 6\overset{\rm m}{.}61$ (see Table 9) this implies a distance in the range from 540 to 1990 pc.

5. The B star HD 32328

Also rather neglected, HD 32328 (BD+43°1177, HIP 23603) is another object close to ε Aur in the sky. It was classified as B8V in an objective prism survey by Duflot et al. (1957) and its only measured RV = +21 km s^{-1} also comes from such a survey (Fehrenbach et al. 1996). It has a rather accurate parallax of $0\overset{''}{.}00612 \pm 0\overset{''}{.}00159$ from the HIPPARCOS mission (van Leeuwen 2007a,b). Deutschman et al. (1976) obtained the following standard *UBV* values

$$V = 7\overset{\rm m}{.}57, \quad B-V = -0\overset{\rm m}{.}04, \quad U-B = -0\overset{\rm m}{.}35,$$

Table 8. Radiative parameters and projected rotational velocity of HD 32328 resulting from the fit of the three Ondřejov spectra with the highest S/N by interpolated synthetic spectra.

RJD	$T_{\rm eff}$ (K)	log g [cgs]	$v \sin i$ (km s^{-1})
56 011.4508	12 891	4.426	44.2
56 013.4003	12 882	4.349	43.8
56 015.2794	12 861	4.278	43.4

Notes. Individual spectra are identified by their reduced Julian dates.

derived $E(B-V) = 0\overset{\rm m}{.}10$ and estimated a distance of 336 pc. For comparison, the measured HIPPARCOS parallax implies a range of distances from 130 to 207 pc.

We obtained 10 red Ondřejov spectra and 10 individual *UBV* observations at Hvar. The Hvar photometry agrees well with that by Deutschman et al. (1976, see Table 9) and our value of the reddening is $E(B-V) = 0\overset{\rm m}{.}056$. The dereddened colours indicate a normal main-sequence object between B7 and B8.

Radial-velocity measurements of the sharp Hα absorption core in our spectra (see Table A.4) show small variations with a full range of 8 km s^{-1} and a possible timescale of 6.8 days. This means that also this object could be a single-line spectroscopic binary seen nearly pole-on (unless the component masses are strongly peculiar), but it is also conceivable that it is a rotating star with uneven brightness distribution or even an unusual pulsating star. The time distribution of our spectral, as well as photometric, observations is unsufficient to test such hypotheses, however. We can only state that no trace of a secondary spectrum is visible, therefore a comparison of the observed and synthetic spectra seems justified.

Since HD 32328 is cooler than the lower $T_{\rm eff}$ limit of the B star grid of synthetic spectra by Lanz & Hubeny (2007), we had to interpolate in the grid of synthetic spectra from the POLLUX database (Palacios et al. 2010), based on Kurucz's models. For the comparison we selected three spectra with the highest signal-to-noise ratios (S/N). The results are summarized in Table 8 and characterize the uncertainty of the fit. The comparison of model fits with these three spectra is shown in Fig. C.2 in Appendix C. Note that without being able to apply KOREL in this case, we could not remove the telluric lines from the observed spectra.

The corresponding evolutionary tracks are shown in Fig. C.5 in Appendix C. They imply a mass between 3.4 and 4.5 $M_\odot$, $M_{\rm bol} = -0\overset{\rm m}{.}49$ to $-1\overset{\rm m}{.}98$, $M_{\rm V} = 0\overset{\rm m}{.}31$ to $-1\overset{\rm m}{.}18$, which with $V_0 = 7\overset{\rm m}{.}475$ (Table 9) implies a distance between 270 and 540 pc. In contrast to it, the range of the distance following directly from the HIPPARCOS parallax is (175 ± 45) pc. The question is whether HD 32328 is not indeed a binary composed from two similarly bright stars observed pole-on. In any case, we use the lower limit of the HIPPARCOS measurements and the upper limit of the spectroscopic distance as the range of possible distances to HD 32328.

6. The B star HD 277197

HD 277197 (BD+43°1161; $V = 9\overset{\rm m}{.}5$) is a little studied B star. It is classified as B1 IV by Bouigue (1959) and B5 by McCuskey (1959) but no MKK classification was published. The only $B-V$ photometry was published by Bouigue (1959), who obtained

$$V = 9\overset{\rm m}{.}51, \quad \text{and} \quad B-V = +0\overset{\rm m}{.}06.$$

Table 9. *UBV* photometry of calibration stars and their dereddened values.

Star	V (mag)	$B-V$ (mag)	$U-B$ (mag)	V_0 (mag)	$(B-V)_0$ (mag)	$(U-B)_0$ (mag)
HD 31617	7.429 ± 0.004	$+0.003 \pm 0.002$	-0.748 ± 0.002	6.612	−0.249	−0.933
HD 32328	7.657 ± 0.004	-0.047 ± 0.003	-0.343 ± 0.002	7.475	−0.103	−0.383
HD 277197	9.495 ± 0.003	$+0.063 \pm 0.002$	-0.547 ± 0.003	8.649	−0.197	−0.737
BD+43°1168	9.395 ± 0.006	$+0.918 \pm 0.007$	$+0.276 \pm 0.004$	6.425	+0.02	−0.56

We secured three red spectra of it with the Onřejov 2-m reflector and 31 individual *UBV* observations during 2011 and 2012 at Hvar.

Since the clouds interrupted the exposure of the first spectrum, it has a $S/N = 42$ only. However, the remaining two are well exposed and permit a comparison with the synthetic spectra. The mean RV of the Hα and He I 6678 Å lines from all three spectra is -3.4 ± 0.7 km s^{-1}, rather similar to both ε Aur and the HD 31894 binary. When comparing the second and third spectra to the synthetic spectra from the B star grid of Lanz & Hubeny (2007, see Fig. C.3 in Appendix C), we found that the best fit is obtained for

$$T_{\rm eff} = 17\,750\,{\rm K},\ \log g = 4.459\,[{\rm cgs}],\ \text{and}\ v \sin s = 44.7\,{\rm km\,s^{-1}}.$$

The differential Hvar *UBV* photometry did not reveal any variability during two seasons. We therefore derived robust mean values from all 31 individual observations to obtain $V = 9\overset{\rm m}{.}495 \pm 0.003$, $B-V = 0\overset{\rm m}{.}063 \pm 0.002$, and $U-B = -0\overset{\rm m}{.}547 \pm 0.003$.

A standard dereddening gives

$$(B-V)_0 = -0\overset{\rm m}{.}197,\ (U-B)_0 = -0\overset{\rm m}{.}737,\ \text{and}\ E(B-V) = 0\overset{\rm m}{.}260.$$

Both the derredened magnitudes and the $T_{\rm eff}$ deduced from the observed spectra agree with a spectral type near B3.

Evolutionary tracks modelling the results of the comparison of the observed and synthetic spectra are shown in Fig. C.6 in Appendix C and imply a mass of 5.5 to 6.7 $M_\odot$, $M_{\rm bol}$ between $-2\overset{\rm m}{.}49$ and $-3\overset{\rm m}{.}50$, $M_{\rm V}$ between $-0\overset{\rm m}{.}92$ and $-1\overset{\rm m}{.}81$ and for $V_0 = 8\overset{\rm m}{.}649$ the spectroscopic distance from 820 to 1230 pc.

7. The field star BD+43°1168

The B9 Iab supergiant BD+43°1168 (ADS 3605E) is the closest to ε Aur in the sky from the stars considered here. The spectral classification was derived by Morgan et al. (1955), while its RV $= -22$ km s^{-1} was measured by Münch (1957). The *UBV* photometry was derived by Hiltner (1956) as

$$V = 9\overset{\rm m}{.}39,\ \ B-V = 0\overset{\rm m}{.}92,\ \ U-B = 0\overset{\rm m}{.}20,$$

while Fernie (1983) obtained

$$V = 9\overset{\rm m}{.}48,\ \ B-V = 0\overset{\rm m}{.}95,\ \ U-B = 0\overset{\rm m}{.}12$$

as a mean of 3 individual observations.

The mean of 9 *UBV* observations secured at Hvar is

$$V = 9\overset{\rm m}{.}395 \pm 0\overset{\rm m}{.}006,$$

$$B-V = 0\overset{\rm m}{.}918 \pm 0\overset{\rm m}{.}007,$$

$$U-B = 0\overset{\rm m}{.}276 \pm 0\overset{\rm m}{.}004.$$

The above three determinations of *UBV* magnitudes differ a bit more than what one would expect. In Fig. 8 we reproduce a part of the better exposed spectrum of the star. From a comparison with a spectrum of another B9Iab star σ Cyg taken with the same instrumentation, one can suspect the presence of a weak emission in the Hα line of BD+43°1168. From analogy with other emission-line stars, a slight secular variability of BD+43°1168 cannot therefore be excluded.

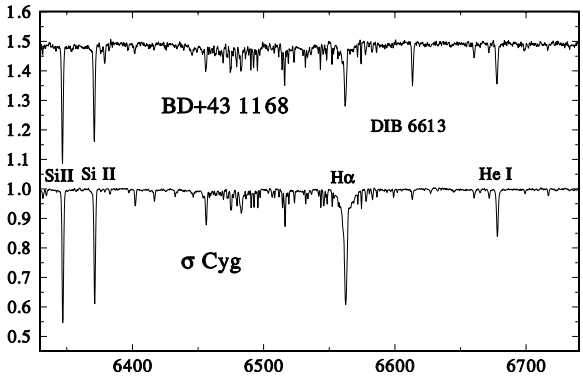

Fig. 8. A comparison of the Ondřejov red spectrum of BD+43°1168 taken on HJD 2 456 008.3159 with a spectrum of another B9Iab star σ Cyg, taken with the same instrumentation and kindly put at our disposal by Dr. M. Kraus. Note the strong 6613.56 Å interstellar line in the spectrum of BD+43°1168 and its faint Hα profile, obviously partly filled by emission.

According to Johnson (1958), the intrinsic colours of a B9Iab supergiant are $B-V = +0\overset{\rm m}{.}02$ and $U-B = -0\overset{\rm m}{.}52$. This implies $E(B-V) = 0\overset{\rm m}{.}90$ for Hiltner's and our Hvar values, and $E(B-V) = 0\overset{\rm m}{.}93$ for the values published by Fernie. From this, one then obtains the derredened V_0 magnitude from formula (1) to be $6\overset{\rm m}{.}39$ and $6\overset{\rm m}{.}37$, repectively. The absolute visual magnitude of a B9Iab supergiant is expected to be $-6\overset{\rm m}{.}2$ (Cox 2000) to $-6\overset{\rm m}{.}4$ (Straizys & Kuriliene 1981), which with the above estimated V_0 range implies a distance to BD+43°1168 between 3.27 and 3.61 kpc.

Our measured value of $EW(6613) = 0.230 \pm 0.020$ Å is in good agreement with a published value of 0.20 Å (Bromage & Nandy 1973).

8. Inferred calibration relations

We plot the distance calibrations based on the data for calibration stars in the neighbourhood of ε Aur in the sky (see Table 10) in Fig. 9. One can see that all three calibrations d(EW), $d(I_{\rm c})$, $d(E(B-V))$ are well-defined and they are consistent with each other:

$$d({\rm EW}) = (1.474 \pm 0.028) \times 10^4\,{\rm EW}, \quad (3)$$

$$d\,(I_{\rm c}) = (-2.027 \pm 0.171) \times 10^4\ (1 - I_{\rm c})\,, \quad (4)$$

$$d(E(B-V)) = (3.888 \pm 0.089) \times 10^3\,E(B-V). \quad (5)$$

Also note that these calibrations are *not* dependent on any outliers. For example, if we drop the most distant star (BD+43 1168) and extrapolate linearly from the remaining data

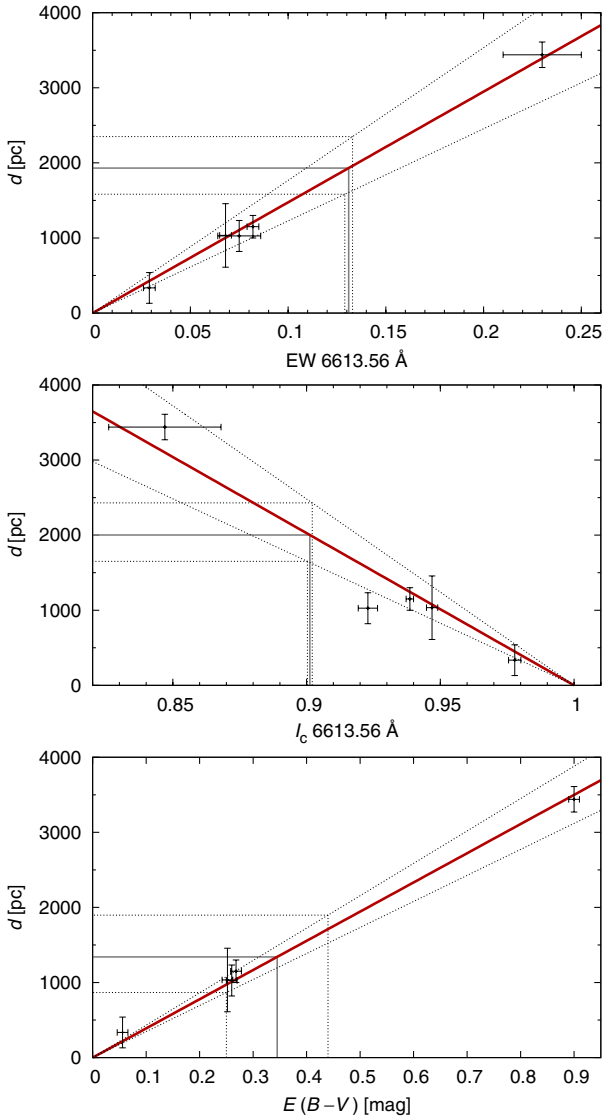

Fig. 9. Calibrations of the distance and a function of the strength of the diffuse interstellar 6613.56 Å line and of the $E(B-V)$ reddening. The solid gray lines show the mean EW, I_c, and $E(B-V)$ values of ε Aur and the corresponding distance, the dotted lines indicate the range of uncertainties.

we would obtain equivalent results for the distances in the 1000 to 2000 pc range.

9. Measured and deduced properties of ε Aur

It is not quite straightforward to derive a reliable reddening of ε Aur since its brightness and colours undergo cyclic physical variations on a time scale of some 50 to 120 days (cf., e.g. Chadima et al. 2011). An inspection of the existing 107 individual Hvar standard *UBV* observations secured prior and after the recent eclipse of ε Aur shows that the observed $B-V$ is in the range between $0\overset{m}{.}51$ and $0\overset{m}{.}57$. Since the true nature of the physical variations is not known, we consider the mean value of $B-V = 0\overset{m}{.}54$ as well as both extremes. There is also some uncertainty regarding the effective temperature of the ε Aur F primary. From a rather detailed line-profile modelling, Bennett et al. (2005) derived 7000 K, while Sadakane et al. (2010) and Chadima et al. (2011) arrived at 8000 K. Modelling the energy distribution, Hoard et al. (2010) used 7750 K for the F primary.

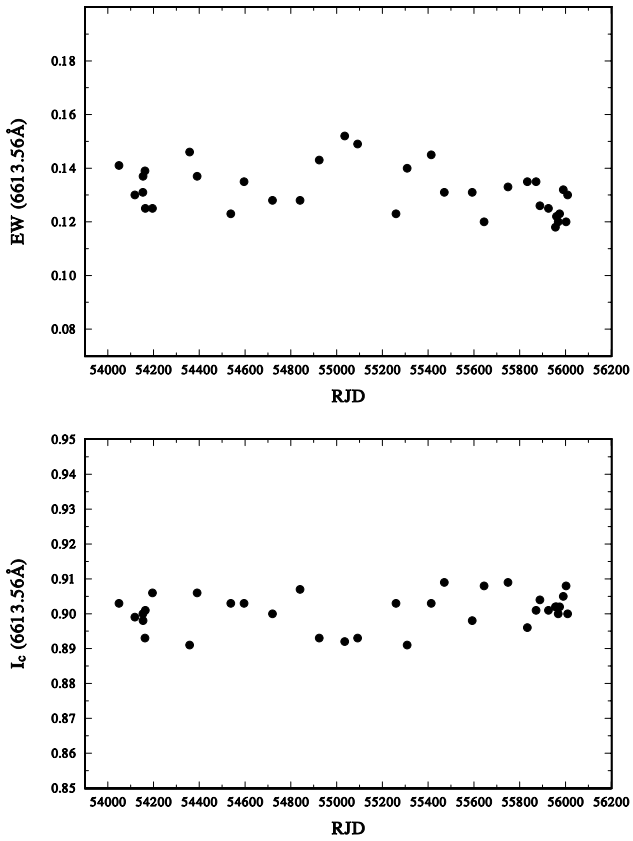

Fig. 10. Time plots of the equivalent width (EW) and central intensity (I_c) of the 6613.56 Å diffuse interstellar line measured on a representative sample of the Ondřejov CCD spectra over the time interval from 2006 to 2012. No significant change during the 2009–2011 primary eclipse (RJD 55 050 to 55 800) is observed, which corroborates the conclusion that the line is of a truly interstellar (not partly cirmcumstellar) origin.

Using again the calibration between the effective temperature and intrinsic $B-V$ colour, one arrives at $(B-V)_0$ between $+0\overset{m}{.}16$ and $+0\overset{m}{.}30$ for the calibration by Flower (1996), while Johnson (1958) gives $(B-V)_0 = +0.23$ for F0I stars. So the total range of $E(B-V)$ to be considered as appropriate for ε Aur is $0\overset{m}{.}25$ to $0\overset{m}{.}44$. It should be noted that a small contribution to the observed reddening could arise from circumbinary dust. However, the large grain size indicated by the models (cf., e.g. Budaj 2011) and lack of variations in the diffuse interstellar band indicate that this contribution is probably insignificant.

We measured the equivalent width (EW) and central intensity (I_c) of the 6613.56 Å diffuse interstellar line in a representative selection of the Ondřejov spectra secured from 2006 to 2012, including the spectra taken during the 2009–2011 eclipse. Both these measured quantities are plotted vs. time in Fig. 10. One can see that there is no noticeable difference in the strength of the line between the eclipse and out-of-eclipse data. This indicates in our opinion that the line is of truly interstellar, not partly circumstellar origin and can be used as a distance indicator.

In Fig. 9 we can see that all three distance calibrations are consistent and put ε Aur very clearly at a distance larger than about 900 pc. Considering the calibration results, we estimate the most probable distance to ε Aur to be about (1500 ± 500) pc. Its uncertainty is mostly caused by the dispersion of I_c and $E(B-V)$ observed for ε Aur.

Table 10. Estimated distances, strength of the 6613.56 Å interstellar line and the $E(B-V)$ reddening for all calibration stars.

Distance	EW 6613 Å	I_c 6613 Å (pc)	$E(B-V)$	Object
0	0	1	0	zero distance
335 ± 205	0.029 ± 0.003	0.9778 ± 0.0023	0.056	HD 32328
1030 ± 210	0.075 ± 0.011	0.9229 ± 0.0036	0.260	HD 277197
1035 ± 420	0.068 ± 0.003	0.9469 ± 0.0021	0.252	HD 31617
1150 ± 150	0.082 ± 0.003	0.9386 ± 0.0014	0.268	HD 31894
?	0.131 ± 0.002	0.9012 ± 0.0009	0.25–0.44	ε Aur
3440 ± 170	0.230 ± 0.020	0.847 ± 0.021	0.90	BD+43 1168

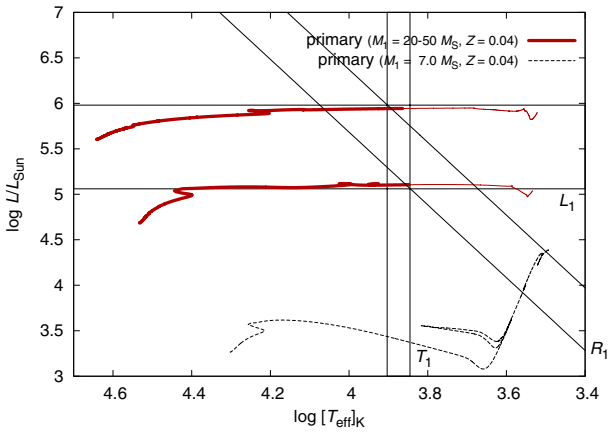

Fig. 11. Evolutionary tracks computed for ε Aur in the HR diagram. We show the evolution from the zero-age main sequence. The thin lines correspond to the observed effective temperatures, radii and luminosities of ε Aur. The range of masses are indicated in the legend. We also plot the evolutionary track for a lower-mass star ($m_{\rm ini}$ = 7 $M_\odot$) for comparison as a dotted line. It never reaches the observed luminosity, even in the post-AGB phase. The post-AGB evolution track (not shown in the plot) is nearly horizontal (at nearly a constant $\log L/L_\odot \sim 4.4$) as the star moves to the hotter (left) in the diagram.

Stencel et al. (2008) derived the angular diameter of the F primary of ε Aur out of eclipse to be between 2.16 and 2.38 mas. For the distance of (1500 ± 500) pc this implies the F star radius of 232 to 512 $R_\odot$. The corresponding range of absolute visual magnitudes of ε Aur is then $M_{\rm V}$ = −7.m9 to −10.m2 mag. This seems to speak in favour of the high-mass model for ε Aur and identifies its primary as a relatively young object.

Indeed, the evolutionary tracks computed by the `MESAstar` module show that the allowed range of masses is 20 to 50 $M_\odot$ (see Fig. 11). We assumed initial helium abundance Y = 0.320 and metallicity Z = 0.040, the mixing-length parameter α = 2.0, scheme for the wind by Reimers (1975) in the red giant branch (RGB) and by Blöcker (1995) in the AGB phase, respectively, with the efficiencies η = 1.0. We used Z = 0.04 for consistency with all investigated calibration (supposedly young) stars since the true evolutionary stage of ε Aur is still not clear. We have verified, however, that the inferred mass range *is not sensitive* to the selected value of metallicity. Even with solar-like values Z = 0.016–0.020 and Y = 0.28, the evolutionary tracks are not significantly different, only the timescale is prolonged by approximately 6%. In this model, the star has evolved away from the main sequence and is in the evolutionary stage when the central hydrogen abundance dropped to zero and the star consequently moves to lower effective temperatures. For the 20 $M_\odot$ star, the star has already ignited the helium in the core so that the change in $T_{\rm eff}$ is much slower than for the 50 $M_\odot$ model. For this reason, we consider the lower mass of 20 $M_\odot$ as more probable than the higher one. Note that the total mass loss is not important yet (less than 1% of the initial mass) and the selected wind parametrisation thus does not affect results significantly.

This is to be compared to the previous results of van Winckel (2003) who estimated the maximum luminosity for post-AGB supergiants, i.e. stars with *initial* masses lower than ∼7 $M_\odot$, to be $\log L/L_\odot \approx 4.4$ ($M_{\rm bol}$ = −6.m2 mag) which is well below the value estimated in this work. We thus conclude that the lower-mass model of ε Aur does not fulfill observational constraints.

Formally, it is also possible to reproduce the observed properties of ε Aur assuming that it is a pre-main sequence star with mass from 30 to 70 $M_\odot$ but this interpretation seems improbable since the evolution is so fast that the changes should be seen in the recorded history of the star, which is not the case (cf., e.g. Johnston et al. 2012).

If the high-mass model is confirmed, the future works should clarify whether the dark disk around the secondary could be formed by a strong wind from the F-supergiant primary. Since the current wind of the F supergiant appears too weak to sustain such a disk, one viable possibility is that prior to becoming an F supergiant, the star could have undergone a luminous blue variable (LBV) phase, in which a carbon rich super-wind was accreted by the secondary star. Note that the revision of the ε Aur distance can have far reaching consequences also on some other results. For instance, the energy distributions derived by Hoard et al. (2010) and Hoard et al. (2012) need to be reconsidered (as also pointed to us by Bennett 2012, priv. comm.).

10. Prospects for future work

Note also that ε Aur is catalogued as a little studied multiple star system (ADS 3605 ABCDE). The components ADS 3605B, C, and D are relatively faint and are located at 23, 45, and 47 arcsec from ADS 3605A = ε Aur and have the V magnitudes of +14.m0, +11.m26, and +12.m0, respectively (Aitken & Doolittle 1932). Because ε Aur lies very close to the galactic plane (b = +1.18°), it is possible that at least one or all of these putative faint components are field stars. For example ADS 3605C = BD+43°1166C has a published $B-V$ = +1.m83 (Lutz & Lutz 1977), which indicates that it may be a dM foreground star[4]. It would be important to secure spectroscopy and *UBV* photometry of these companions to determine if any of them is a physical companion to ε Aur. This would provide a more definite distance check. No doubt the observations of these close companions

[4] The differential *UBV* observations of this star secured at Hvar (12 individual observations in 5 nights) give V = (10.m927 ± 0.m090), $B-V$ = 0.m714 ± 0.m021, and $U-B$ = 0.m319 ± 0.m012. However, these observations were challenging and strongly require independent verification.

to ε Aur will be challenging due to the brightness of ε Aur itself ($V \simeq +3\overset{m}{.}0$). (In the field of the 2-m telescope, these stars have always been outshone by ε Aur itself and obtaining their spectra there is out of the question.) But their observations could readily be accomplished with current equipment using adaptive optics, coronagraph-equipped telescopes or interferometric nulling methods used for exoplanets. It would be worth the effort to learn more about the distance to ε Aur and, consequently about its true nature.

In conclusion, the present study offers strong (but circumstantial) evidence that ε Aur is at a distance of 1.0–2.0 kpc. This favours a high luminosity and radius for the F-supergiant and therefore supports ε Aur as being a massive binary system, younger than about 7×10^6 yr. Note that additional arguments supporting this interpretation were recently provided by Johnston et al. (2012). But nothing seems to come easy in the study of ε Aur. And as the concluding remarks of many previous papers on ε Aur typically state: *More work is needed to finally unravel numerous mysteries and puzzles of this fascinating and intriguing eclipsing binary.*

Acknowledgements. We are grateful to Dr. H. Lehmann, who kindly obtained and reduced one echelle spectrum of HD 31894 for us, to Dr. A. H. Batten, who communicated to us the exact mid-exposure times of the four older DAO photographic spectra of HD 31894, and to Dr. Michaela Kraus for her permission to show here a plot of 1 Ondřejov spectrogram of σ Cyg, which she obtained. We acknowledge the use of the public version of the programs FOTEL and KOREL written by Dr. P. Hadrava and the grid of synthetic spectra of B stars made publicly available by Hubeny and Lanz. We thank an anonymous referee for the tough but justified, fair and constructive criticism of the first version of this study and additonal useful suggestions to the second version, which led us to re-do the whole paper and hopefully strengthen the arguments in favour of a larger distance to ε Aur. Useful discussions on the subject with Dr. S. S. Shore are also gratefully acknowledged. We profitted from the use of the bibliography maintained by the NASA/ADS system and the CDS in Strasbourg. The Czech authors were supported by the grant P209/10/0715 of the Czech Science Foundation and also from the research programs AV0Z10030501 and MSM0021620860. The US authors are very grateful for support of this work from NASA Grants NNX09AAH28G + GO-12302.01 and NSF/RUI Grants AST-0507542 + AST-1009903.

References

Adams, W. S., & Joy, A. H. 1917, ApJ, 46, 313
Aitken, R. G., & Doolittle, E. 1932, New general catalogue of double stars within 120 of the North pole, Carnegie institution of Washington, Washington, D.C.
Bennett, P. D., Ake, T. B., & Harper, G. M. 2005, BAAS, 37, 495
Blöcker, T. 1995, A&A, 297, 727
Bouigue, R. 1959, Annales de l'Observatoire Astron. et Meteo. de Toulouse, 27, 47
Bromage, G. E., & Nandy, K. 1973, A&A, 26, 17
Budaj, J. 2011, A&A, 532, L12
Carnochan, D. J. 1986, MNRAS, 219, 903
Carroll, S. M., Guinan, E. F., McCook, G. P., & Donahue, R. A. 1991, ApJ, 367, 278
Chadima, P., Harmanec, P., Yang, S., et al. 2010, IBVS, 5937, 1
Chadima, P., Harmanec, P., Bennett, P. D., et al. 2011, A&A, 530, A146
Cox, A. N. 2000, Allen's Astrophysical Quantities, 4th edition, ed. by A. N. Cox (New York: AIP Press and Springer)
Danziger, I. J., Wallerstein, G., & Böhm-Vitense, E. 1967, ApJ, 150, 239
Deutschman, W. A., Davis, R. J., & Schild, R. E. 1976, ApJS, 30, 97
Dobashi, K., Uehara, H., Kandori, R., et al. 2005, PASJ, 57, 1
Duflot, M., Fehrenbach, C., Guillaume, J., & Ray, G. 1957, Publications of the Observatoire Haute-Provence, 4, 11
Eggleton, P. P., & Pringle, J. E. 1985, ApJ, 288, 275
Fehrenbach, C., Duflot, M., Genty, V., & Amieux, G. 1996, Bulletin d'Information du Centre de Données Stellaires, 48, 11
Fernie, J. D. 1983, ApJS, 52, 7
Flower, P. J. 1996, ApJ, 469, 355
Galazutdinov, G. A., LoCurto, G., & Krełowski, J. 2008, ApJ, 682, 1076
Guinan, E. F., & DeWarf, L. E. 2002, in Exotic Stars as Challenges to Evolution, eds. C. A. Tout, & W. van Hamme, ASP Conf. Ser., 279, 121
Hadrava, P. 1990, Contributions of the Astronomical Observatory Skalnaté Pleso, 20, 23
Hadrava, P. 1995, A&AS, 114, 393
Hadrava, P. 1997, A&AS, 122, 581
Hadrava, P. 2004a, Publ. Astron. Inst. Acad. Sci. Czech Rep., 92, 1
Hadrava, P. 2004b, Publ. Astron. Inst. Acad. Sci. Czech Rep., 92, 15
Hadrava, P. 2005, Ap&SS, 296, 239
Harmanec, P., Horn, J., & Juza, K. 1994, A&AS, 104, 121
Heintz, W. D., & Cantor, B. A. 1994, PASP, 106, 363
Hiltner, W. A. 1956, ApJS, 2, 389
Hoard, D. W., Howell, S. B., & Stencel, R. E. 2010, ApJ, 714, 549
Hoard, D. W., Ladjal, D., Stencel, R. E., & Howell, S. B. 2012, ApJ, 748, L28
Hobbs, L. M., York, D. G., Thorburn, J. A., et al. 2009, ApJ, 705, 32
Horn, J., Kubát, J., Harmanec, P., et al. 1996, A&A, 309, 521
Jenniskens, P., & Desert, F.-X. 1994, A&AS, 106, 39
Johnson, H. L. 1958, Lowell Observatory Bulletin, 4, 37
Johnson, H. L. 1965, ApJ, 141, 923
Johnston, C., Guinan, E. F., Harmanec, P., & Mayer, P. 2012, in AAS Meeting Abstracts, 219, 153.34
Koornneef, J. 1983, A&A, 128, 84
Kuiper, G. P., Struve, O., & Strömgren, B. 1937, ApJ, 86, 570
Lambert, D. L., & Sawyer, S. R. 1986, PASP, 98, 389
Lanz, T., & Hubeny, I. 2007, ApJS, 169, 83
Ludendorff, H. 1903, AN, 164, 81
Lutz, T. E., & Lutz, J. H. 1977, AJ, 82, 431
McCall, B. J., Drosback, M. M., Thorburn, J. A., et al. 2010, ApJ, 708, 1628
McCuskey, S. W. 1949, ApJ, 109, 414
McCuskey, S. W. 1959, ApJS, 4, 1
Morgan, W. W., Code, A. D., & Whitford, A. E. 1955, ApJS, 2, 41
Munari, U., Tomasella, L., Fiorucci, M., et al. 2008, A&A, 488, 969
Münch, G. 1957, ApJ, 125, 42
Palacios, A., Gebran, M., Josselin, E., et al. 2010, A&A, 516, A13
Paxton, B., Bildsten, L., Dotter, A., et al. 2011, ApJS, 192, 3
Perryman, M. A. C., & ESA. 1997, The HIPPARCOS and TYCHO catalogues (Noordwijk, Netherlands: ESA Publications Division), ESA SP Ser., 1200
Petrie, R. M., & Lee, E. K. 1966, Publ. Dom. Astrophys. Obs. Victoria, 12, 435
Petrie, R. M., & Pearce, J. A. 1961, Publ. Dom. Astrophys. Obs. Victoria, 12, 1
Plaskett, J. S., & Pearce, J. A. 1931, Publ. Dom. Astrophys. Obs. Victoria, 5, 1
Prša, A., & Zwitter, T. 2005, ApJ, 628, 426
Prša, A., & Zwitter, T. 2006, Ap&SS, 304, 347
Reimers, D. 1975, Mem. Soc. Roy. Sci. Liege, 8, 369
Sadakane, K., Kambe, E., Sato, B., Honda, S., & Hashimoto, O. 2010, PASJ, 62, 1381
Savage, B. D., Massa, D., Meade, M., & Wesselius, P. R. 1985, ApJS, 59, 397
Schlegel, D. J., Finkbeiner, D. P., & Davis, M. 1998, ApJ, 500, 525
Škoda, P. 1996, in Astronomical Data Analysis Software and Systems V, ASP Conf. Ser. 101, 187
Stefanik, R. P., Torres, G., Lovegrove, J., et al. 2010, AJ, 139, 1254
Stencel, R. E., Creech-Eakman, M., Hart, A., et al. 2008, ApJ, 689, L137
Straizys, V., & Kuriliene, G. 1981, Ap&SS, 80, 353
Strand, K. A. 1959, AJ, 64, 346
Torres, G. 2010, AJ, 140, 1158
van de Kamp, P. 1978, AJ, 83, 975
van de Kamp, P., & Lippincott, S. L. 1968, AJ, 73, 781
van Leeuwen, F. 2007a, in Astrophysics and Space Science Library (Springer), 350
van Leeuwen, F. 2007b, A&A, 474, 653
van Winckel, H. 2003, ARA&A, 41, 391
Walborn, N. R. 1971, ApJS, 23, 257

Pages 12 to 15 are available in the electronic edition of the journal at http://www.aanda.org

Appendix A: Details of spectroscopic observations and their analyses

With one exception, all spectra used in this study were secured in the coudé focus of the Ondřejov 2.0-m reflector and a 702-mm focal length camera with a SITe-005 800 × 2000 CCD detector covering the wavelength region 6260–6760 Å. The spectra have a linear dispersion 17.2 Å mm^{-1} and a 2-pixel resolution $R \sim 12\,600$ (~11–12 km s^{-1} per pixel). With one exception, their S/N is at least 100 or better. The journal of observations of all stars is in Table A.1.

Table A.1. Journal of spectral observations of ε Aur and the calibration stars in its neighbourhood.

Star	No. of. spectra	Time interval (RJD)
ε Aur	280	54 049.4–55 913.3
HD 31617	10	55 959.4–56 043.3
HD 31894	19	55 578.4–55 692.3
HD 32328	10	55 960.3–56 043.3
HD 277197	3	55 821.4–55 837.5
BD+43°1168	2	55 976.4–56 008.3

Table A.2. Individual RVs of HD 31894 for the primary from the old photographic spectra and the RVs of the primary and secondary from the new electronic spectra measured via Gaussian fits.

RJD	RV$_1$ (km s^{-1})	RV$_2$ (km s^{-1})	Obs.
26 276.9788	–44.0	–	DAO
31 749.0048	13.0	–	DAO
34 297.9639	–5.0	–	DAO
34 735.7704	1.0	–	DAO
55 578.4268	19.6	–35.9	OND
55 602.3073	–116.2	191.4	OND
55 618.3613	31.1	–46.1	OND
55 618.4995	28.7	–48.4	OND
55 619.5146	29.8	–65.1	OND
55 622.4573	22.3	–47.5	OND
55 623.4108	–29.2	53.6	OND
55 631.2495	36.1	–68.0	OND
55 635.2864	–131.6	213.9	OND
55 642.2977	34.7	–68.5	OND
55 642.4187	37.5	–68.4	OND
55 644.3406	30.1	–53.6	OND
55 651.2891	26.0	–44.3	OND
55 661.3810	17.3	–34.3	OND
55 662.3785	21.4	–52.7	OND
55 670.3250	–13.8	22.9	TLS
55 671.3145	+6.3	–16.9	OND
55 672.2947	+13.4	–34.2	OND
55 692.3364	–14.7	25.7	OND

Notes. The reduced heliocentric Julian dates RJD = HJD – 2 400 000 are tabulated.

For HD 31894, one echelle spectrogram (4700–7085 Å, 2-pixel resolution of 63 000) was kindly obtained for us by Dr. Holger Lehmann with the Tautenburg Observatory 2-m reflector on JD 2 455 670.3. Dr. Lehmann also kindly carried out the initial reductions of that spectrogram (bias subtraction, flat-fielding, order merging and wavelength calibration) in IRAF. Similar initial reductions of all Ondřejov spectrograms were carried out by MŠ, also in IRAF. The final reductions and RV measurements were carried out by PH in the program SPEFO, written by the late Dr. J. Horn and further developed by Dr. P. Škoda and Mr. J. Krpata (Horn et al. 1996; Škoda 1996). In SPEFO, one derives the RVs via sliding the direct and flipped image of a line profile until a perfect match is obtained. We also measured a selection of good telluric lines to use them to a fine correction of the RV zero point for each spectrogram. After these corrections, the final RVs for HD 31894 were derived via a Gaussian fit of the He I 6678 Å line profile by PM. All individual RVs of HD 31894 are in Table A.2.

Table A.3. Individual DAO and Ondřejov RVs of HD 31617.

RJD	RV (km s^{-1})	rms (km s^{-1})
24 064.9953	4.80	–
25 614.8008	3.40	–
25 621.6945	8.30	–
25 642.7182	–2.40	–
55 959.4293	12.64	0.23
55 970.5035	–0.88	0.34
55 976.3167	–1.91	0.31
56 008.3733	–15.47	0.21
56 009.3183	–15.14	0.47
56 012.3213	–15.29	0.30
56 013.3368	–14.86	0.19
56 015.3163	6.50	0.42
56 041.3434	–5.57	0.12
56 043.3126	–3.60	0.33

Notes. The RVs on the Ondřejov CCD spectra were measured in SPEFO and each value is the mean of the RVs of the following four lines: Hα 6562.817 Å, He I 6678.151 Å, C II 6578.052 Å, and C II 6582.882 Å. The reduced heliocentric Julian dates RJD = HJD – 2 400 000 are tabulated.

Table A.4. Individual Ondřejov RVs of HD 32328 measured in SPEFO on the sharp core of Hα.

RJD	RV (km s^{-1})
55 960.3317	10.68
55 970.2849	7.73
56 008.4007	12.02
56 009.2846	9.18
56 011.4508	12.24
56 012.4020	14.91
56 013.4003	14.28
56 015.2794	10.85
56 041.3848	13.05
56 043.3463	13.54

Notes. The reduced heliocentric Julian dates RJD = HJD – 2 400 000 are tabulated.

Appendix B: Photometry

The calibrated Hvar *UBV* observations of ε Aur and all calibration stars were obtained differentially relative to the comparison star λ Aur, used as the primary comparison by most observers of ε Aur. HR 1644 served as the check star. All observations

Table B.1. Journal of *UBV* observations of ε Aur and the calibration stars in its neighbourhood.

Star	No. of. obs.	Time interval (RJD)	Note
ε Aur	334	45 307.5–56 015.3	1
HD 31617	13	56 001.3–56 015.3	1
HD 31894	87	55 574.3–55 858.7	1
	120	55 629.7–55 665.6	2
HD 32328	10	56 001.3–56 015.3	1
HD 277197	31	55 791.6–56 015.3	1
BD+43°1168	9	56 001.3–56 013.3	1

Notes. 1... Hvar; 2... Villanova APT.

were carefully reduced to the standard Johnson system via non-linear transformation formulae (Harmanec et al. 1994) using the latest rel.17 of the program HEC22[5]. The more recent versions of HEC22 allow monitoring and modelling the variations of the atmospheric extinction during observing nights. The following mean Hvar all-sky values for λ Aur were added to the respective magnitude differences var-comp and check-comp:

$V = 4\overset{\mathrm{m}}{.}706,\quad B-V = 0\overset{\mathrm{m}}{.}619,\quad U-B = 0\overset{\mathrm{m}}{.}143.$

The Villanova APT differential *UBV* observations of HD 31894 were secured relative to HR 1644 and reduced via a standard APT pipeline. The standard Hvar all-sky values for HR 1644

$V = 6\overset{\mathrm{m}}{.}224,\quad B-V = 0\overset{\mathrm{m}}{.}451,\quad U-B = 0\overset{\mathrm{m}}{.}334.$

were added to the magnitude differences var-comp. The journal of photometric observations is in Table B.1.

Appendix C: Model fits

Here, we present a comparison of the disentangled spectrum of HD 31617 and the observed spectra of HD 32328 and HD 277197 with the best-fit interpolated synthetic spectra in Figs. C.1–C.3, respectively. For the same stars, we also show the evolutionary tracks calculated in such a way to fit the $T_{\rm eff}$ and log g deduced from the observed spectra – see Figs. C.4–C.6, respectively.

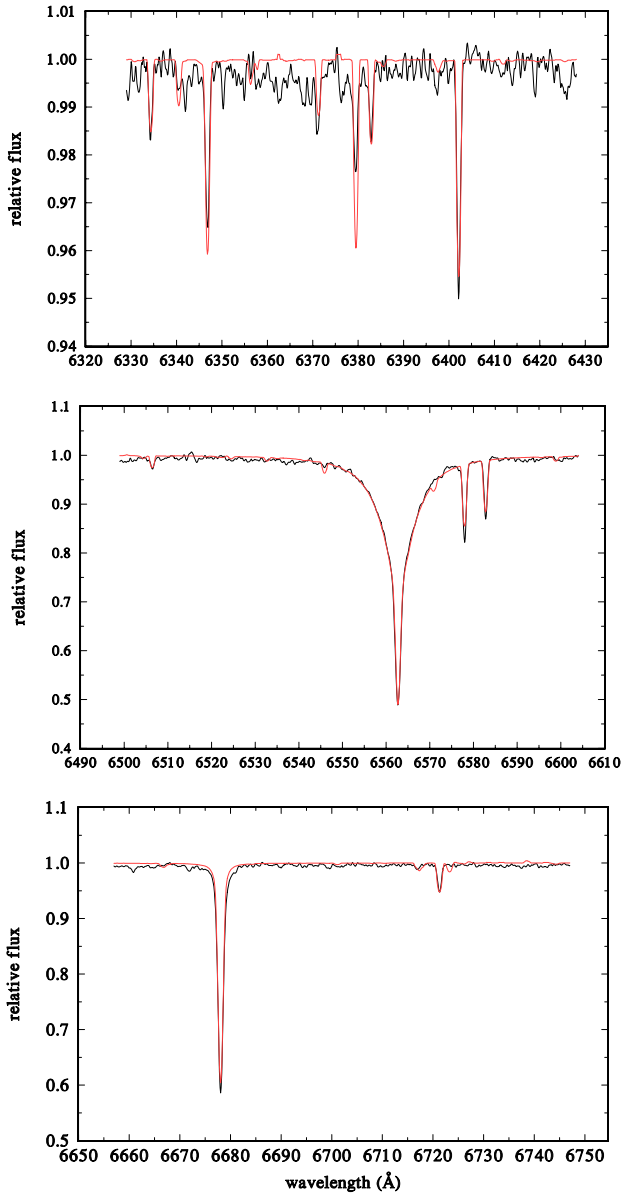

Fig. C.1. A comparison of the disentangled red spectrum of HD 31617 (black lines) with the model spectrum (red lines).

[5] The whole package containing the program HEC22 and other programs for complete photometric reductions, sorting and archiving the data, together with a very detailed User manual, is freely available at http://astro.troja.mff.cuni.cz/ftp/hec/PHOT.

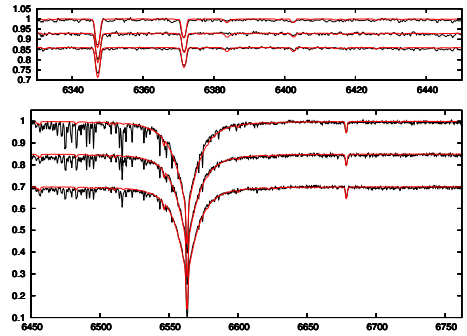

Fig. C.2. A comparison of three individual Ondřejov spectra of HD 32328 (black lines) having the highest S/N with the model spectra (red lines). From top to bottom, the spectra were taken on RJD 56 011.4508, 56 013.4003, and 56 015.2794, respectively. Note that we could not remove the telluric lines from the observed spectra in this case.

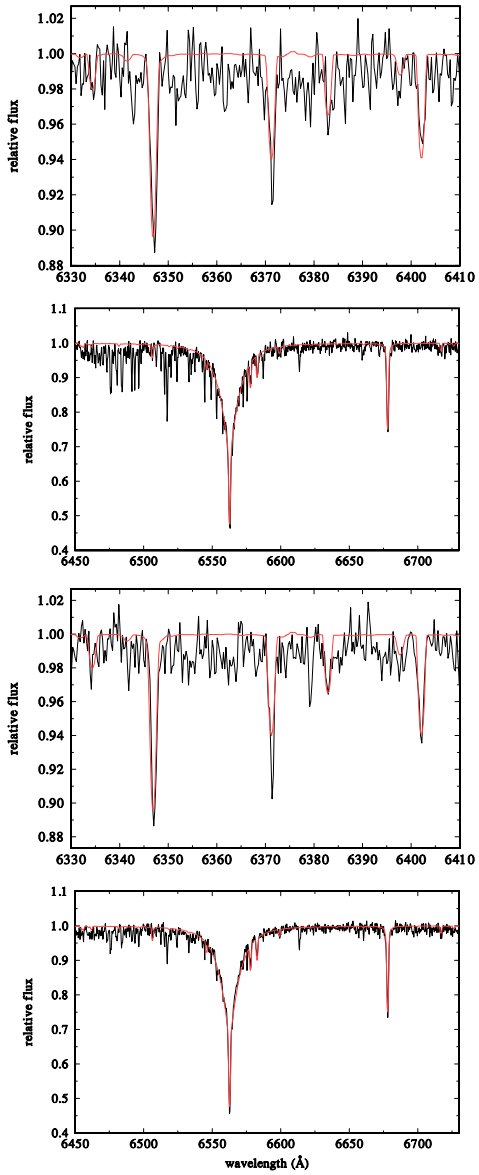

Fig. C.3. A comparison of two individual Ondřejov spectra of HD 277197 (black lines) with the model spectra (red lines). From top to bottom, the spectra were taken on RJD 55 833.4303 (*top* two plots) and RJD 55 837.4985 (*bottom* two plots). Note that the telluric and interstellar lines were not removed from the observed spectra in this case.

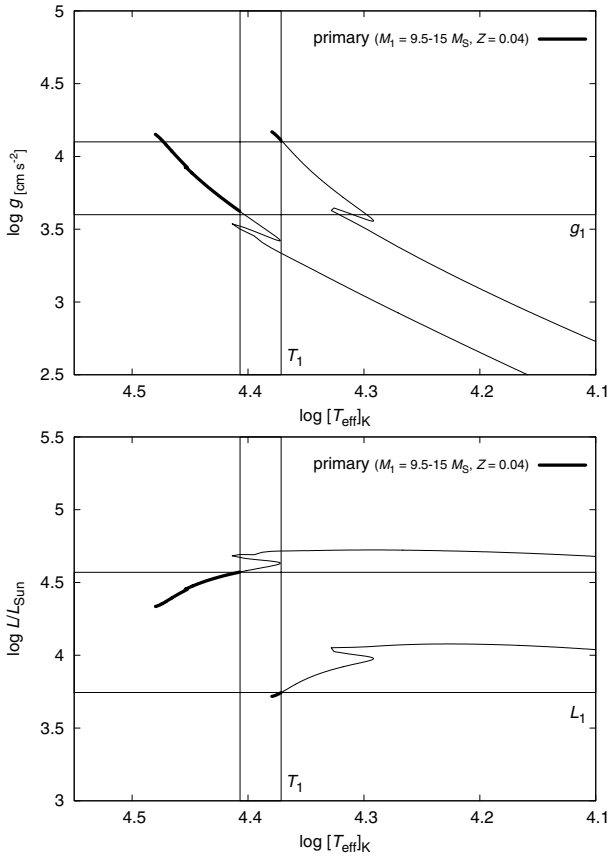

Fig. C.4. Computed evolutionary tracks of the primary of HD 31617 in a log g vs. $T_{\rm eff}$ diagram and in the HR diagram. See the text for details.

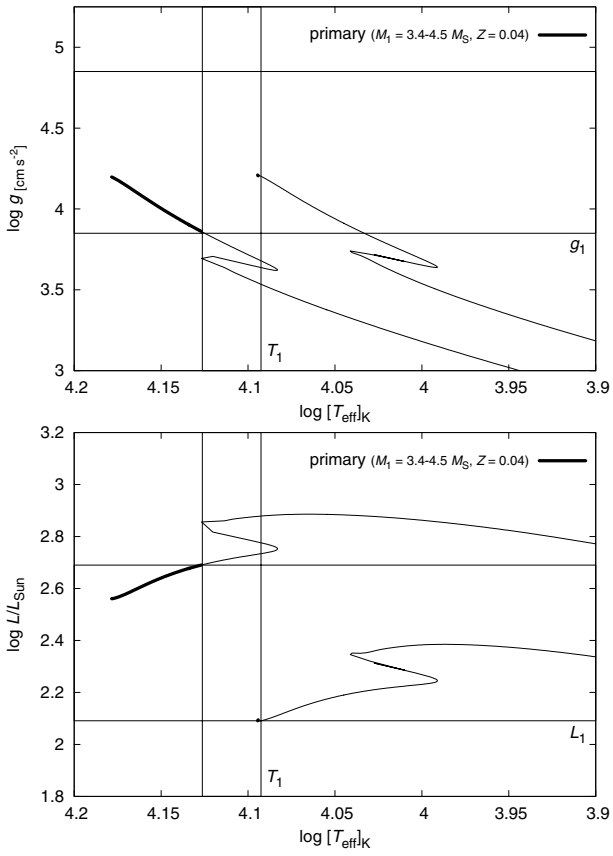

Fig. C.5. Computed evolutionary tracks of HD 32328 in a log g vs. $T_{\rm eff}$ diagram and in the HR diagram. See the text for details.

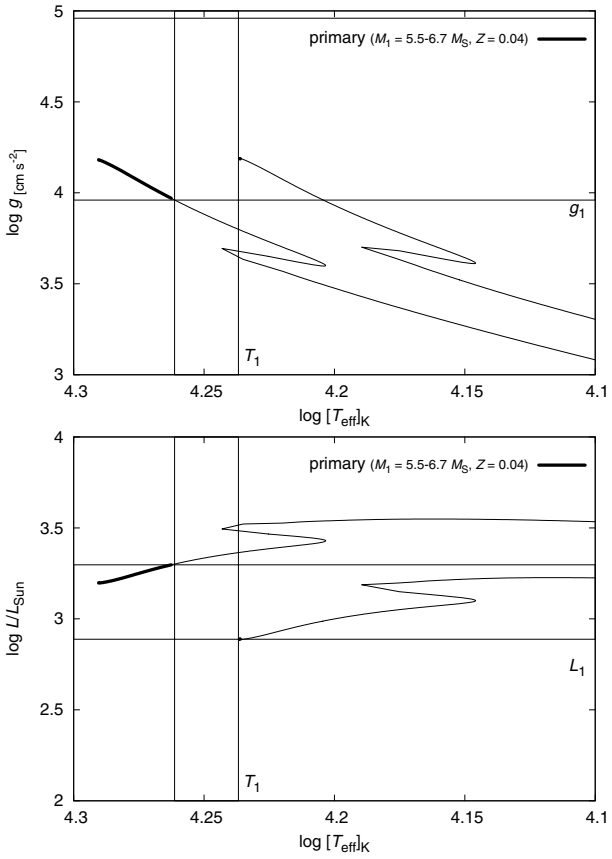

Fig. C.6. Computed evolutionary tracks of HD 277197 in a log g vs. $T_{\rm eff}$ diagram and in the HR diagram. See the text for details.